Experimental study of fracture surface roughness on rocks with crack velocity

Franck Plouraboué,[1,2] Kenneth W. Winkler,[3] Luc Petitjean,[3] Jean-Pierre Hulin,[2] and Stéphane Roux[1]
[1]*Laboratoire de Physique et de Mécanique des Milieux Hétérogènes, Ecole Supérieure de Physique et Chimie Industrielles de Paris, 10 rue Vauquelin, 75231 Paris Cedex 05, France*
[2]*Laboratoire Fluides, Automatique et Systèmes Thermiques, Batiment 502, Université de Paris-Sud, 91405 Orsay, France*
[3]*Schlumberger-Doll Research Center, Old Quarry Road, Ridgefield, Connecticut 06877*
(Received 17 July 1995)

In this paper we address the question of the influence of crack velocity on the fractured surface roughness. We studied samples made of Berea sandstone, chosen for their good macroscopic homogeneity and their granular microstructure. The samples were fractured in a double cantilever geometry, which allowed for a controlled crack speed that was maintained constant for each sample using an imposed displacement quadratic in time. The range of speed covered in the experiments was 5×10^{-4} m s^{-1} to 2×10^{-1} m s^{-1}. Systematic profilometry measurements of the fractured surfaces revealed a self-affine geometry characterized by a roughness exponent, which was found to be independent of the crack speed.

PACS number(s): 02.50.−r

I. INTRODUCTION

Trivially enough, the fracture surface of heterogeneous materials is rough. However, somewhat unexpectedly, the roughness of the surface *is not* a mere perturbation of a regular surface at the scale of the microstructure. On the contrary, fractography analyses reveal systematically a very broad spectrum of length scales over which roughness is significant. Generally, the largest length scales (up to the sample size) contribute dominantly to the overall roughness. Moreover, spectral analyses or other techniques show [1–4] that the topography of the surface displays a scale-invariant character, known as "self-affinity" [5]. There is now very abundant literature which reports on such a property for many materials, with different mechanical properties and fracture conditions. The objective of the present work is to investigate the dependence of this roughness on the crack velocity for experiments performed on sandstone samples.

Self-affinity is characterized by a single exponent ζ — known as the Hurst or roughness exponent — which governs the scale transformation that leaves invariant the topography of the fracture surface in a statistical sense. An outstanding feature is the fact that in most cases all measured values of ζ are similar [6]. Being careful with the estimate of error bars in the determination of ζ which are often underestimated [7], the reported values are generally consistent with the claim for universality of the roughness exponent which was first suggested by Bouchaud *et al.* [8] from experimental analyses. In three dimensions, $\zeta \approx 0.8 \pm 0.05$.

Asserting universality from experimental data is a very difficult task. From the theoretical side this self-affine character and *a fortiori* its eventual universality still constitute a challenging question waiting for a satisfactory explanation. However, considering the variety of materials which have been studied as well as the large scale difference between microscopic features and the largest roughness features, the scaling invariance has to be the result of fairly general considerations only marginally dependent on any precise material property. However, some changes have been reported [9] in the roughness statistics based on different tests performed on Ti_3Al-based super α_2 alloy at different speeds (which were ranked but not measured). This observation partly motivates our study, first because this may shed light on the origin of self-affinity, and second because of practical applications of these results (such as increasing the permeability enhancement in hydraulic fracturing). Let us discuss in more detail these two motivations.

Several approaches seem appealing in searching both for an explanation of the self-affine property and for a possible sensitivity to crack speed.

(a) *A dynamical instability.* For some "homogeneous" materials it has long been known that fracture roughness is related to the crack propagation velocity. This is a well known [see [10] for poly methyl metacrylate (PMMA)] observation for glass where the succession of mirror-mist-hackle patterns is commonly related to the crack velocity. Detailed nanoscopic analysis reveals that in fact, although such a classification is convenient, the roughness *continuously* increases with the distance to the initiation point, and, moreover, very local measurements reveal mirrorlike regions inside the mist and hackle zones, and similarly mistlike regions in the hackle zone [11]. This qualitative scaling invariance conforms with the idea of self-affine roughness. Quantitative profilometry on PMMA sheets also shows that the roughness over a fixed window scale is a simple function of the mean crack speed over this window [12]. It is, however, to be noted that those cases concern high crack velocities, i.e., a significant fraction of the Rayleigh wave speed.

(b) *A change of mechanism.* For some materials (glass,

ceramics, etc.) the variation of the stress intensity factor with the crack speed [13,14] reveals two domains, a controlled propagation regime which depends crucially on the environment (humidity, temperature, etc.) and which is believed to be a stress-induced corrosion at the crack tip, and a fast propagation regime which is independent of the environment. The transition between these two regimes through an increase of the speed is generally associated with a drastic increase of the roughness. Again these regimes are separated by a threshold velocity, which in contrast with the previous mechanism may be much lower than the Rayleigh wave speed (and dependent on the environmental conditions). Nanoscopic topography analyses performed on glass at very low crack velocities show a self-affine nature of these surfaces, in the range of length scales from 1 nm to 1 μm, characterized, however, by a value of the roughness exponent ($\zeta \approx 0.5$) [11] much lower than the one observed on other materials generally at a much larger scale above 1 to 10 μm.

(c) *A statistical roughening due to microstructural heterogeneities.* Inspired by statistical models, it is tempting to draw a comparison between the crack roughness and interfaces obtained in growth models which can be modeled by Langevin equations in a noisy environment. In the case of fracture, the Langevin equation would be simply the crack front motion equation supplemented by a short-range correlated noise which accounts for the microstructure. Famous examples of such Langevin equations includes the Edwards-Wilkinson model or the Kardar-Parisi-Zhang equation ([15–17] for recent reviews). They naturally give rise to self-affine geometries. Such a parallel has been recently suggested by Bouchaud and Bouchaud [18] with an annealed noise. Moreover, the growth of the roughness of a crack starting from a straight notch, analyzed experimentally on granite samples, displays a scaling form similar to the one expected in such a model [19]. It is, however, to be noted that starting from the initial notch the crack is expected to accelerate so that the dependence on the distance may as well be a dependence on the velocity.

A velocity dependence may arise from these models when a quenched noise is taken into account. This dependence has a specific form. It appears progressively starting from a zero velocity, and at a nonzero velocity one expects a small-scale regime which corresponds to the quasistatic case, and a large-scale regime much more comparable with the annealed noise behavior. The crossover scale which divides these two regimes is a correlation length which is expected to decrease with velocity.

Thus we see that a systematic study of the roughness as a function of the crack velocity may give information on the mechanism at play which is responsible for the crack morphology.

Besides this fundamental interest for studying the influence of the crack velocity on the fractured surface roughness, there has also long existed a practical interest in fracturation. Rock fracturation is, for instance, of interest in domains as varied as hydrology, civil and petroleum engineering, and geothermal processes [20]. Hydraulic fracturation has been used now for 40 years to increase well productivity (i.e., the hydraulic permeability of wells). The classical fracturation velocity is small (typically $= 10^{-5}$ m s^{-1}), but this technique does not allow for a permanent gain of productivity. A new technique called overbalanced perforation [21], developed recently, seems promising in attaining durable productivity gains. Rock fracturation is achieved by pressurizing water in the bore hole head by a column of gas in the well. This new fracturation method reaches higher fracturation speeds (typically $v = 1$ m s^{-1}). Previous works of the same authors have shown the influence of the roughness of a crack surface on the aperture between both faces of the crack [22,23]. The roughness exponent is shown to be a key parameter governing variations of both the aperture and the hydraulic permeability. This context provides a good motivation for a systematic investigation of the dependence of roughening on the crack velocity.

We have performed a systematic study of the influence of the crack velocity on the roughness of Berea sandstone samples, with precise control of the fracturation process and careful measurement of the fracture speed. We shall first describe in Sec. II the sample characteristics and the fracturation method. We will then examine in Sec. III the roughness characterization with profilometry measurements and its interpretation.

II. SAMPLE CHARACTERISTICS AND FRACTURATION METHOD

Berea sandstone is a well-known and well-studied rock. It is also a good model for homogeneous grained brittle rock. We use Berea sandstone samples, macroscopically homogeneous, composed of very compact sand grains of 10 μm to 100 μm in size. The hydraulic permeability of the samples is 500 mdarcy. The sample dimensions are $2l \times l \times 10l$ (7.8 cm×3.4 cm×34 cm), used in order to avoid boundary influences on the fracturation process along the large axis. Hence the fracturation direction is parallel to the large axis, horizontal, and parallel to the sedimentation bed of the sandstone. A 7-cm-long horizontal slit at one of the ends of the sample is initially sawn to provide a double cantilever beam geometry and act as an initiation notch (cf. Fig. 1). Fracturation is kept

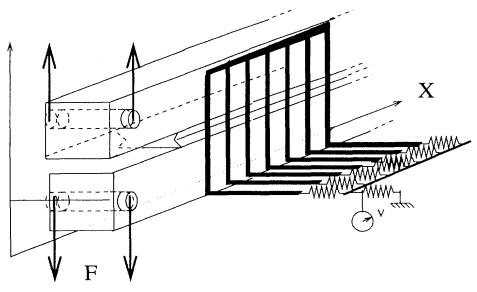

FIG. 1. Double cantilever Berea sandstone beams of dimensions 7.8 cm×3.4 cm×34 cm are fractured horizontally, imposing a vertical displacement $y(t)$. A conductive comb allows an electrical transduction of the temporal evolution of the crack tip location.

in the horizontal plane by two lateral guiding notches, a few millimeters deep. A mode I fracture is induced by a controlled relative vertical displacement across the initiation notch using a computer-controlled tensile testing device. Displacement is imposed every 5×10^{-2} s with a 50 μm accuracy and maximum vertical speed of 4 mm s^{-1}. Velocity measurements of the crack tip are provided by electrical transducers. Fragile tissue paper is glued on each lateral sample side. Using standard silk screen techniques, a 3.4 mm periodic comb was laid onto the tissue paper with a conductive (silver suspension) ink (cf. Fig. 1). Connecting each tooth with an electrical resistance allows electrical transduction of the temporal variation of the crack front evolution. This technique permits one to estimate the speed with an accuracy better than 10%.

The vertical displacement was chosen to be quadratic in time so that the crack velocity should remain constant. A simple justification is provided by the following elementary computation. Let us introduce the elastic modulus E and inertia momentum I of the section of one beam. Let d be the distance between the applied force F and the crack tip. The relative vertical displacement y of the two grip points is

$$y = \frac{2Fd^3}{3EI}. \tag{1}$$

Assuming no torque is exerted on the grips, and calling M_c the value of the flexural moment which produces the critical stress intensity factor at the crack tip, we write

$$y(t) = \frac{2M_c}{3EI} d(t)^2. \tag{2}$$

Constant velocity of the crack front during fracturation $d(t) \propto tv$ requires a quadratic variation of the vertical displacement $y(t)$ with time:

$$y(t) \propto \frac{2M_c v^2}{3EI} t^2 \propto At^2. \tag{3}$$

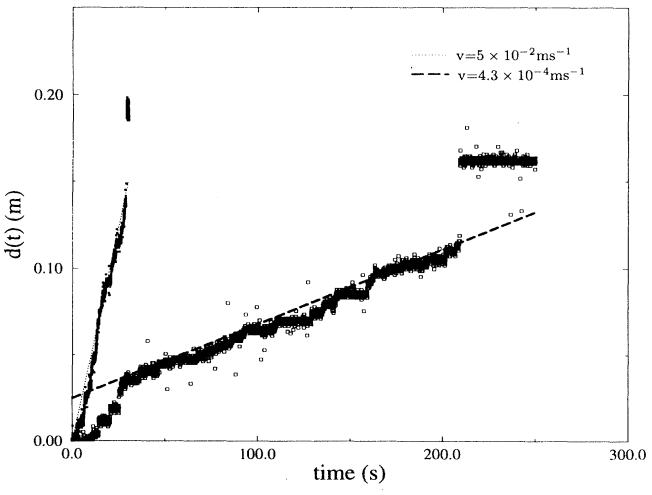

FIG. 2. Temporal evolution $d(t)$ of the crack tip reconstructed from electric signal by linear calibration. Two different experiments are shown; the velocity of the crack is estimated by the straight lines as $v_1 = 5.0 \times 10^{-2}$ m s^{-1} and $v_2 = 4.3 \times 10^{-4}$ m s^{-1} with 10% accuracy.

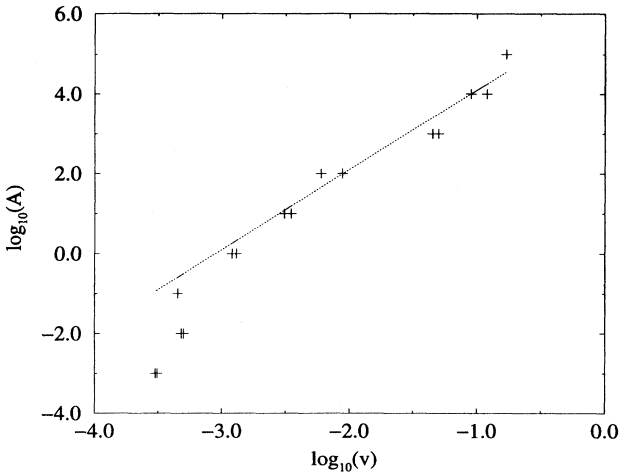

FIG. 3. Measured crack velocity v is shown as a function of the acceleration of the grips in log-log coordinates. The predicted variation is shown as a straight line. Symbol size is bigger than experimental uncertainty.

The parameter A can be controlled experimentally. Figure 2 shows the electric signal of the linear variation of the crack front $d(t)$ with time, recorded with the said imposed displacement. Constant crack velocity can then be obtained over horizontal distances greater than 10 cm with very good accuracy. Figure 3 shows the scaling $A \propto v^2$ of A with v, and the reproducibility of the crack velocity from one sample to another in the same fracturation conditions. The upper cutoff of the scaling is due to the vertical speed limitation of the tensile testing device. Hence the minimum and maximum speeds obtained were $v_{min} = 5 \times 10^{-4}$ m s^{-1} and $v_{max} = 2 \times 10^{-1}$ m s^{-1}, for a total of 30 fractured samples, all velocities being small compared to the Rayleigh speed v_R ($v_{max}/v_R \approx 10^{-4}$).

III. ROUGHNESS ANALYSIS

A careful observation of the fractured surfaces shows the existence of branched structures on the lateral sides of most samples. However, in the central part of the samples, the surface topography does not present such irregularities. The fracturation speed v is constant over 10 cm during the fracturation process, and much lower than the critical velocity v_c of the branching regime, so that we conclude that the observed branchings are only due to the presence of the boundary. We therefore focus our interest on the roughness over a 1-cm-wide and 10-cm-long region in the central part of the fracture surface oriented along the crack propagation direction.

A. Profilometry measurements

Roughness has been characterized using mechanical profilometry. The vertical height of a profile is mea-

sured by a probing contact tip that follows continuously the sample surface during the motion of a translating arm. Angular deviations of the arm due to vertical displacement of the probing tip are transduced into self-inductance variations. Data are collected when the speed of the probe is stabilized. Vertical and horizontal displacement accuracy as well as the repeatability were of a few micrometers. Good reproducibility, up to a few micrometers, is obtained for sandstone, indicating no induced damage to the sample surfaces. Although good accuracy is obtained for absolute variations of the probing tip, we will see in the next section that the probe geometry has a significant influence on the reliability of the measurements. We performed experimental profilometry measurements over 18 sandstone samples, corresponding to the different fracturation velocities. For each sample, 20 profiles, 4 cm long and with a 15 μm sampling period, were collected along 10 cm in the region of constant fracture velocity. Then data were analyzed through standard analysis techniques to reveal a potential self-affine character: power spectra analyses, the variable bandwidth method, and the first return probability method.

B. Data analysis

We focus our interest here on the monofractal aspect of the surface geometry. Multifractal characterization of fractured surfaces could also have been addressed [24] although it requires a very high quality of the measurements and rather large statistics to reach definitive conclusions. Moreover, the physical application of such characterization remains mostly to be exploited. Several techniques allow the measurement of the roughness exponent from profilometry data [7]. The most standard means is to study the power spectrum. One has to compute the Fourier transform $\tilde{z}(k)$ of the profiles $z(x)$, and construct the power spectrum $P(k) = |\tilde{z}(k)|^2$ which for self-affine profiles of roughness exponent ζ is expected to scale as

$$P(k) \propto k^{-1-2\zeta}. \tag{4}$$

Averaging $P(k)$ over different profiles preserves the scaling and allows for a more precise determination of the exponent.

Figure 4 shows the averaged power spectrum in log-log coordinates computed from three experimental data sets recorded on samples fractured with extreme and median fracturation velocity: $v = 1.3 \times 10^{-1}$ m s^{-1}, 8.8×10^{-3} m s^{-1}, and 3.0×10^{-4} m s^{-1}. The most striking feature of this graph is the perfect superposition of the spectra obtained for surfaces corresponding to different fracturation velocities. This observation will be confirmed by the other analyses and constitutes the main conclusion of our study. Fitting the spectrum by a power law as expected if the surface is self-affine provides the estimate of the roughness exponent $\zeta = 0.75$. However, it is also obvious from the figure that the power-law behavior is not completely satisfactory. In the following, we will discuss a possible cause of alteration of the profile due to the shape of the probe used in the profilometry.

Another way of revealing a self-affine character is the variable bandwidth method which consists in dividing a given profile of length L into windows of width Δ. The standard deviation of the height, σ, and the difference δ between the maximum and minimum height are computed on each band, and averaged over all windows of given width Δ covering the total length L from the origin, $\langle\sigma\rangle_\Delta$ and $\langle\delta\rangle_\Delta$. Window sizes larger than $L/2$ are discarded because of insufficient independent sampling. Both quantities follow, due to self-affine invariance, the simple scaling

$$\langle\sigma\rangle_\Delta \propto \Delta^\zeta, \tag{5a}$$

$$\langle\delta\rangle_\Delta \propto \Delta^\zeta. \tag{5b}$$

Figure 5 represents the averaged mean standard deviation of the height $\langle\sigma\rangle$ for a bandwidth Δ versus Δ in

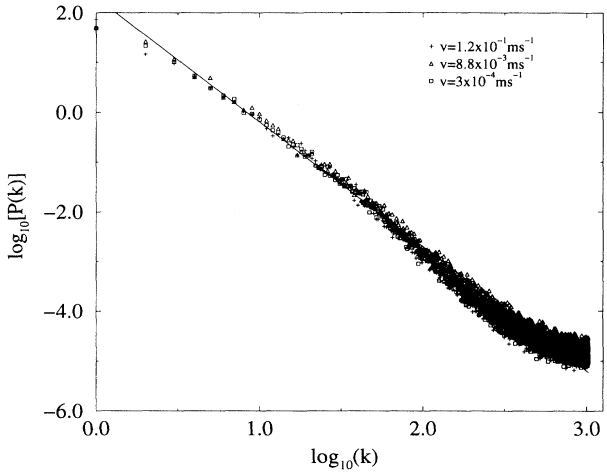

FIG. 4. Experimental averaged power spectra computed from 20 profiles of size 2048 points. A straight line corresponding to a roughness exponent $\zeta = 0.75$ is shown. Three samples fractured with different velocity $v = 1.3 \times 10^{-1}$, 8.8×10^{-3}, and 3.0×10^{-4} m s^{-1} cannot be distinguished.

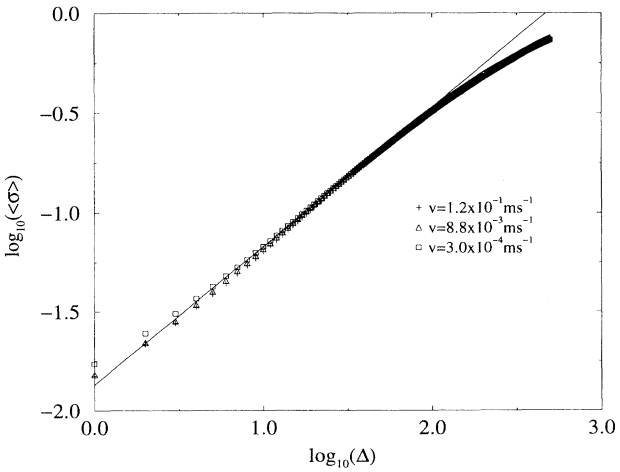

FIG. 5. Variable bandwidth method is used to analyze profilometry data. Root mean square deviation σ is plotted versus the window size Δ and shown for the same data as in Fig. 4. A straight line corresponding to $\zeta = 0.7$ is shown. A good superposition is obtained as in Fig. 4.

log-log coordinates for the same data as in Fig. 4. The scaling of Eq. (5a) is followed over two decades and allows for an estimation of the roughness exponent $\zeta = 0.7$. Figure 6 represents the averaged difference between the minimum and the maximum of the height $\langle\delta\rangle$ versus the window size Δ in log-log coordinates for the same data as in Figs. 4 and 5. The data follow the power law expected from Eq. (5b) over two decades and provides the estimate $\zeta = 0.85$. Reference [24] has shown that finite size effects for 2048 sample sizes lead one to underestimate the roughness exponent with the mean standard deviation method and slightly overestimate it with the min-max method. The power spectrum method is expected to be rather accurate for such system sizes.

Finally, we use a third method to analyze the profiles, the first return probability method. It consists in computing the probability distribution $p(d)$ for the profile to reach the same height at distance d. More precisely, if for each point x_0 the profile height is $h(x_0)$ then one has to determine the minimum distance d at which the profile is intersected again at the same height $h(x_0 + d) = h(x_0)$. The distribution of distances d for all the points of the profile is called the first return probability $p(d)$, and satisfies, for self-affine profiles [25],

$$p(d) \propto d^{\zeta-2}. \tag{6}$$

Figure 7 illustrates the scaling of Eq. (6) for the first return probability distribution $p(d)$ with distance d. One can see, for the same data as in Figs. 4, 5, and 6, a very good superposition of different sets. However, this method appears in the present case to provide a rather poor determination of the roughness exponent.

The accuracy and reliability of these different methods are discussed in detail in [24] and [25], taking into account finite size effects, intrinsic measurement uncertainty, and experimental artifacts. We have estimated, in this study, the influence of the probing tip on the reliability of the

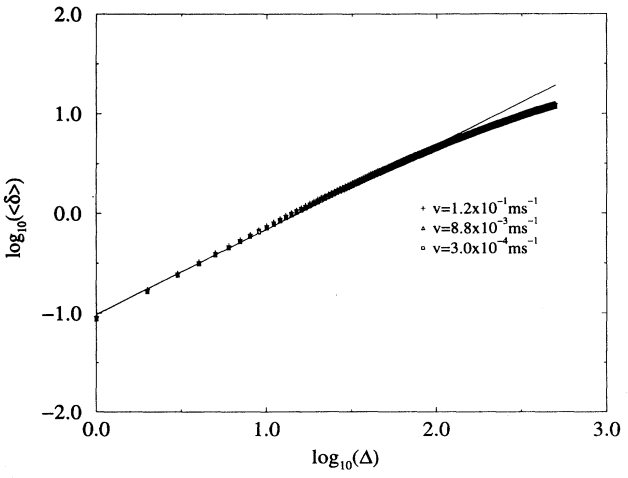

FIG. 6. Variable bandwidth method is used to analyze profilometry data. Min-max difference δ is plotted versus the window size Δ and shown for the same data as in Fig. 4. A straight line corresponding to $\zeta = 0.85$ is shown. A good superposition is obtained as in Fig. 4.

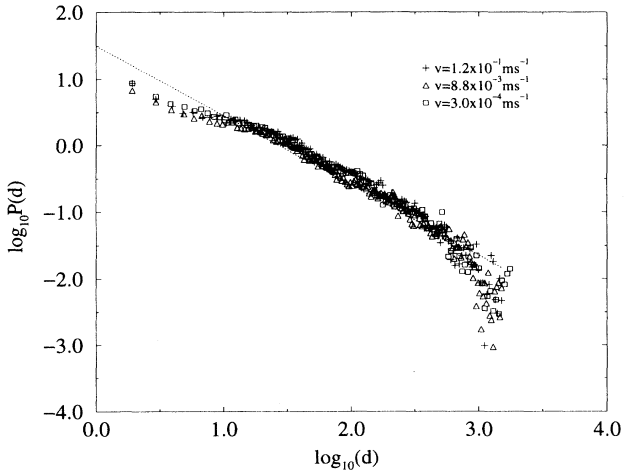

FIG. 7. First return method is used to analyze profilometry data. The distribution $p(d) \propto d^{2-\zeta}$ is shown in log-log coordinates. A good superposition is obtained as in Figs. 4–6. The straight line shows the best fit to a power law with a roughness exponent $\zeta = 0.9$.

determination of ζ. Due to the finite size of the probing needle, holes are much more difficult to identify than hills, and the recorded profile is partially distorted. In order to quantify this influence, one can compute, starting from an ideal self-affine profile, the "measured" profile, taking into account the geometric constraints, the "shadowing effect," due to the probe shape. Figure 8 shows the conic geometry of the probing needle, which has 45° inclination, and a minimum extreme radius of 13 μm, as well as two rescaled computer generated profiles. The short dashed curve is a self-affine profile generated with an inverse Fourier transform method [26,5]. The long dashed one is the "measured" profile, calculated from the pre-

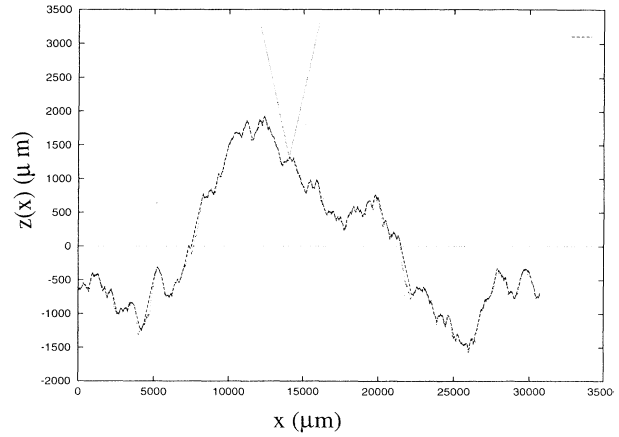

FIG. 8. Profilometry probing tip is shown in real units with a self-affine computer generated profile (both coordinates are expressed in μm with the same characteristics as the experimental profile). The dotted curve corresponds to the rescaled self-affine profile. The dashed line is the modified profile obtained by "measuring" with the profilometer tip the simulated profile (shadowing). These modifications are important for length scales lower than 300 μm.

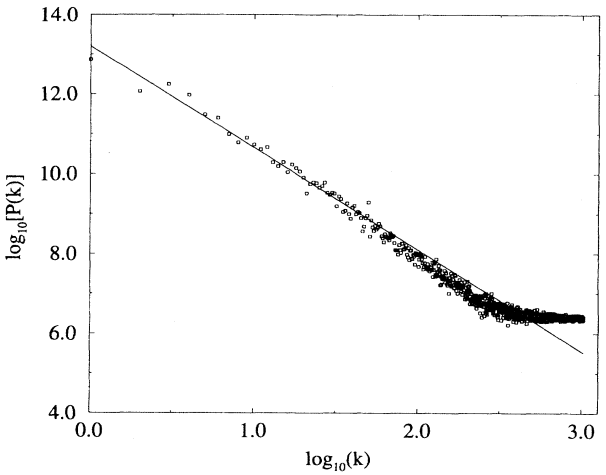

FIG. 9. Power spectra computed from the transformed computer generated profiles of Fig. 8. One can see that the probing tip is acting as a spatial filter of length scales smaller than 300 μm.

vious one taking into account the shadowing. One can see that the difference between the two profiles is small in amplitude but it concerns long regions, far beyond the step size used in the measurement (a few μm), i.e., hundreds of micrometers.

Transforming self-affine generated profiles as in Fig. 8 we show in Fig. 9 the obtained averaged power spectrum of 20 such "measured" profiles of 2048 point size represented in log-log coordinates. This figure indicates that the probe tip is "filtering"out length scales lower than 300 μm, and leads us to consider that significant length scales of our measurements range between 3 cm and 300 μm. Comparison of the resulting spectra with the straight line corresponding to the simulated roughness exponent shows that the spatial filtering of the probe tip leads to a slight overestimation of the measured roughness exponent.

IV. DISCUSSION

Combining the various estimates of the exponent ζ quoted above, together with the systematic bias which results from the shadowing effect, and the very good superposition of data analysis, leads us to conclude that no dependence of the roughness on the crack velocity has been observed. Returning to the possible approaches previously suggested to address the question of fracture roughness, one can make the following observations.

(a) For dynamical instability, the observed stability of the roughness for the experimental range of fracturation speed where $v \ll v_{Rayleigh}$ does not allow us to conclude on this point.

(b) For a change in mechanism, the insensitivity of experimental results to atmospheric humidity gives support to the hypothesis that there is no change of mechanism of the fracturation process when the the crack speed increases, even for very low fracturation speeds.

(c) For microstructure influence, even if we did not observe a dynamical transition that could be linked to the influence of microstructure disorder (described as "quenched noise"in the quasistatic regime and annealed noise in the dynamic regime), such a transition may occur at still smaller fracturation velocities.

These results seem also to imply that, as far as roughness is concerned, all permeability enhancement techniques (hydraulic fracturation for low crack velocity and overbalance perforation for higher fracturation speed) should give similar results.

V. CONCLUSION

We have carried out a systematic investigation of the crack velocity influence on the surface roughness of Berea sandstone samples. Precisely controlled fracturation processes and careful measurement of the crack speed were carried out for a speed range from $v = 1.2\times10^{-1}$ m s^{-1} to $v = 3.0 \times 10^{-4}$ m s^{-1}. Profilometry analysis shows very good reproducibility for all investigated methods and for all data collected on different samples fractured with different speeds. This leads to the conclusion that fracturation speed has no influence on the roughness exponent in the investigated range of velocity fracturation. Systematic investigation of the roughness exponent shows a good agreement with the "universal" value $\zeta = 0.80 \pm 0.05$.

ACKNOWLEDGMENTS

We wish to thank C. Scholz and T. Koszynski from the Lamont Earth Observatory, where the profilometry was done. F.P. acknowledges the support of the Schlumberger Doll Research Center where the fracture experiments were performed. We wish to thank L. McGowan for his help, and E. Bouchaud, B. Couet, H. J. Herrmann and J. Schmittbuhl for useful discussions. The "Laboratoire de Physique et Mécanique des Milieux Hétérogènes" is "Unité de Recherche Associée au CNRS" No. 857. The "Laboratoire Fluide Automatique et Systèmes Thermiques" is "Unité de Recherche Associée au CNRS" No. 871.

[1] B. L. Cox and J. S. Y. Wang, Fractals **1**, 87 (1993).
[2] K. J. Måløy, A. Hansen, E. L. Hinrichsen, and S. Roux, Phys. Rev. Lett. **3**, 213 (1992).
[3] C. Y. Poon, R. S. Sayles, and T. A. Jones, J. Phys. D **25**, 1269 (1992).
[4] S. R. Brown, Geophys. Res. Lett. **14**, 1095 (1987).
[5] J. Feder, *Fractals* (Pergamon Press, New York, 1988).
[6] J. P. Bouchaud, E. Bouchaud, G. Lapasset, and J. Planès, Phys. Rev. Lett. **71**, 2240 (1993).
[7] J. Schmittbuhl, J. P. Vilotte, and S. Roux, Phys. Rev. E **51**, 131 (1995).
[8] E. Bouchaud, G. Lapasset, and J. Planès, Europhys.

Lett. **13**, 73 (1990).
[9] E. Bouchaud and S. Navéos, J. Phys. (France) I **5**, 547 (1995).
[10] V. Auzias, T. Rives, and J. Petit, C. R. Acad. Sci. Paris II **317**, 705 (1993).
[11] M. Guilloteau (private communication).
[12] J. F. Boudet, S. Ciliberto, and V. Steinberg, Europhys. Lett. **30**, 337 (1995).
[13] M. F. Kanninen and C. H. Popelar, *Fracture Mechanics* (Cambridge University Press, New York, 1986), p. 233.
[14] B. R. Lawn and T. R. Wilshow, *Fracture of Brittle Solids* (Cambridge University Press, New York, 1974), p. 103.
[15] T. Halpin-Healy, Phys. Rev. A **42**, 711 (1990).
[16] P. Meakin, Phys. Rep. **235**, 189 (1993).
[17] T. Halpin-Healy and Y. C. Zhang, Phys. Rep. **254**, 215 (1994).
[18] E. Bouchaud and J. P. Bouchaud, Phys. Rev. E **50**, 17752 (1994).
[19] J. Schmittbuhl, Y. Berthaud, and S. Roux, Europhys. Lett. **28**, 585 (1994).
[20] K. J. Evans, T. Kohl, R. J. Hopkirk, and L. Rybach, Technical Report No. 359 to the "Swiss National Energy Research Fund," 1992 (unpublished).
[21] L. Petitjean and B. Couet, Ridgefield Schlumberger-Doll Research Center, Technical Report No. ISD0029401a, 1994 (unpublished).
[22] F. Plouraboué, P. Kurowski, J. Hulin, S. Roux, and J. Schmittbuhl, Phys. Rev. E **51**, 1675 (1995).
[23] S. Roux, J. Schmittbuhl, J. P. Vilotte, and A. Hansen, Europhys. Lett. **23**, 277 (1993).
[24] J. Schmittbuhl, F. Schmitt, and C. Scholtz, J. Geophys. Res. **100**, 5953 (1995).
[25] A. Hansen, C. Poirier, J. P. Troadec, K. J. Maløy, S. Roux, and E. L. Hinrichsen (unpublished).
[26] R. F. Voss, *in Fundamental Algorithms in Computer Graphics*, edited by R. A. Earnshaw (Springer-Verlag, Berlin, 1985), pp. 805–835.